

Crystal Structure of the Alcoholates and the Ansovate of PNU-97018, an Angiotensin II Receptor Antagonist

Hiroaki ISHII,*^a Kentaro YAMAGUCHI,^b Hiroko SEKI,^b Shigeru SAKAMOTO,^b Yuichi TOZUKA,^c Toshio OGUCHI,^c and Keiji YAMAMOTO^c

^aPharmaceutical Sciences, Pharmacia K.K.; 3-20-2 Nishi-Shinjuku, Shinjuku-ku, Tokyo 163-1448, Japan; ^bChemical Analysis Center, Chiba University; 1-33 Yayoi-cho, Inage-ku, Chiba 263-8522, Japan; and ^cGraduate School of Pharmaceutical Sciences, Chiba University; 1-33 Yayoi-cho, Inage-ku, Chiba 263-8522, Japan.

Received November 29, 2001; accepted May 17, 2002

The title compound, PNU-97018 {systemic name: 2-butyl-3,6,7,8,9,11-hexahydro-6,9-dimethyl-3- $\{2'-(2H\text{-tetrazol-5-yl})[1,1'$ -biphenyl]-4-yl\}methyl}-6,9-ethano-4*H*-imidazo[4,5-*d*]-pyridazino[1,2-*a*]pyridazin-4-one} is a newly developed angiotensin II receptor antagonist. The compound and its methanolate and ethanolate were characterized by X-ray crystallography and thermal analysis. The methanolate and ethanolate crystals have an almost identical molecular conformation and crystal packing. In both alcoholates, each alcohol molecule is fixed to the compound with a molar ratio of 1 : 1 by a hydrogen bond between the hydroxyl group of the alcohol molecule and the tetrazole group of the compound. The hydroxyl group of each alcohol molecule further links with the imidazole ring of the neighboring compound by hydrogen bond to form a hydrogen-bond network in both alcoholates. A tunnel-like structure that includes alcohol molecules is formed in each alcoholate. The ansovate crystal showed completely different thermal and X-ray crystallographic characteristics from the alcoholates, where the compound molecules were directly linked by hydrogen bonds between the tetrazole group of a molecule and the imidazole ring of the neighboring molecule. The position of the hydrogen atom in the tetrazole ring was different between the ansovate and alcoholates. Unlike alcoholates, a layer structure stacked on the *b*—*c* plane was observed in the ansovate crystal. It was concluded that the molecular conformation and the arrangement of the compound molecules were largely different between ansovate and alcoholate crystals.

Key words PNU-97018; X-ray crystal analysis; methanolate; ethanolate; molecular conformation; hydrogen bonding

PNU-97018, 2-butyl-3,6,7,8,9,11-hexahydro-6,9-dimethyl-3- $\{2'-(2H\text{-tetrazol-5-yl})[1,1'$ -biphenyl]-4-yl\}methyl}-6,9-ethano-4*H*-imidazo[4,5-*d*]-pyridazino[1,2-*a*]pyridazin-4-one (the compound), is a nonpeptide angiotensin II (A II) receptor antagonist that has insurmountably high antihypertensive activity.^{1,2} A biphenyl tetrazole moiety is the common structure among most nonpeptide A II receptor antagonists such as losartan,³ CV-11194,⁴ D-8731,⁵ L-158809,⁶ and A-81988.⁷ Shin *et al.*⁸ and Heo *et al.*⁹ also studied the molecular structure of their own compounds in this class and demonstrated the differences in the overall conformation of the biphenyltetrazole moiety as well as in its relative orientation with respect to the central heterocyclic fused ring compared with those of some related compounds, indicating that this class of compound has considerable conformational flexibility. Intermolecular hydrogen bonding or any other intermolecular interaction could determine the conformation around the biphenyl linkage in the crystalline state. Since alcohols have hydrogen bonding capability, it is anticipated that alcoholate crystals of this class of compound may possess different molecular conformations than the compound from the corresponding ansovate crystal. In the present investigation, the effect of alcohol solvation on the molecular and crystal structure of the compound was investigated.

Experimental

Materials The compound (Fig. 1) was obtained from Pharmacia K.K. (Tokyo, Japan), and other materials and solvents were of analytical reagent grade. The ansovate crystal of the compound was crystallized from the ethyl acetate solution of the compound. The methanolate and ethanolate crystals were crystallized from the compound solutions in methanol and ethanol, respectively.

X-Ray Structure Determination Clear prismatic crystals of the anso-

vate, methanolate, and ethanolate with approximate dimensions of 0.5×0.25×0.25 mm³, 0.5×0.45×0.45 mm³, and 0.45×0.35×0.20 mm³, respectively, were mounted on a glass fiber. The temperatures for measurements were −95±1 °C for ansovate¹⁰ and −170±1 °C for both methanolate and ethanolate. All measurements were recorded on a CCD area detector (Bruker Smart 1000, Bruker AXS, Madison, WI, U.S.A.) with graphite monochromated MoK α radiation. The structures were solved by direct methods (SIR97)¹¹ and optimized using Fourier techniques (DIRDIF94).¹² The structures were refined by full-matrix least-squares procedures. The nonhydrogen atoms were refined using anisotropic displacement parameters. Hydrogen atoms were included but not refined. The position of the hydrogen atom in the tetrazole ring was confirmed by the electron density. All calculations were performed using the teXan crystallographic software package (teXan for Windows 1997, Molecular Structure Corporation).¹³ The measurement conditions and structural details are listed in Table 1. The final atomic coordinates and the equivalent isotropic thermal displacement parameters were deposited with the Cambridge Crystallographic Data Centre.¹⁴

Differential Scanning Calorimetry Differential scanning calorimetry (DSC) (Pyris 1 differential scanning calorimeter, Perkin-Elmer, Norwalk, CT, U.S.A.) was performed under a N₂ gas flow of 20 ml/min. Samples of about 4 mg in open aluminum pans were heated from 50 to 250 °C at a heat-

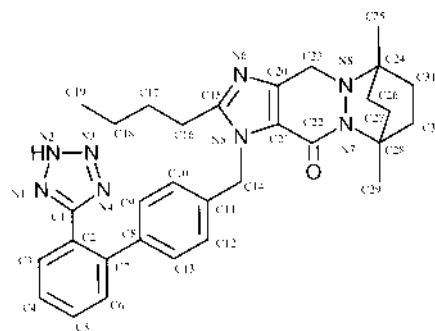


Fig. 1. Chemical Structure of PNU-97018 with Labeling of the Nonhydrogen Atoms

* To whom correspondence should be addressed. e-mail: hiroaki.ishii@pharmacia.com

Table 1. Crystallographic Parameters of PNU-97018 Methanolate, Ethanolate, and Ansolvate Crystals

Crystal	PNU-97018 methanolate	PNU-97018 ethanolate	PNU-97018 ansolvate
Formula	C ₃₂ H ₄₀ N ₈ O ₂	C ₃₃ H ₄₂ N ₈ O ₂	C ₃₁ H ₃₆ N ₈ O
Formula weight	568.72	582.75	536.68
Crystal system	Triclinic	Triclinic	Monoclinic
<i>a</i> (Å)	10.303(2)	10.430(2)	14.297(2)
<i>b</i> (Å)	11.882(2)	12.108(2)	12.722(2)
<i>c</i> (Å)	12.609(2)	12.378(2)	15.353(2)
α (°)	83.241(2)	82.622(3)	90
β (°)	79.387(2)	79.558(3)	90.444(3)
γ (°)	87.592(3)	85.675(3)	90
<i>V</i> (Å ³)	1506.3(4)	1522.3(5)	2792.3(7)
Space group	P $\bar{1}$ (#2)	P $\bar{1}$ (#2)	P2 ₁ /c(#14)
<i>Z</i>	2	2	4
<i>D</i> _c (g/cm ³)	1.254	1.271	1.277
Total no. of reflections measured	9067	9133	16722
No. of unique reflections	6597	6616	6688
No. of observations	4134	3896	2684
Reflection/parameter ratio	10.9	10.0	7.1
<i>R</i> factor	0.038	0.042	0.054
<i>R</i> _w factor	0.047	0.051	0.076
Goodness of fit	1.050	1.130	1.370
2 θ _{max} (°)	56.8	56.8	56.7
Temperature (°C)	-170	-170	-95

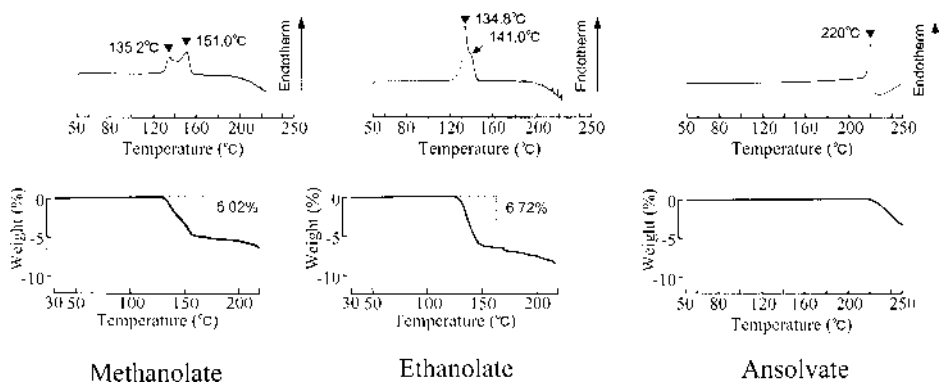


Fig. 2. DSC and TG Profiles of PNU-97018 Methanolate, Ethanolate, and Ansolvate

ing rate of 5 °C/min.

Thermal Gravimetry Thermal gravimetry (TG-DTA model 2000 thermal gravimeter, MAC Science, Yokohama, Japan) was used under a N₂ gas flow of 60 ml/min. Samples of about 6 mg in a platinum pan were heated from 30 or 50 to 230 or 250 °C at a heating rate of 5 °C/min.

Infrared Spectrometry Infrared spectra were recorded on a JASCO model 230 FT/IR spectrometer. The samples were ground with potassium bromide and compressed to obtain disks, and the spectra were recorded at resolution of 4 cm⁻¹.

Results and Discussion

Thermal Behavior of the Ansolvate and Alcohates

Rod-shaped short prismatic crystals were obtained for ansolvate, while thick prismatic crystals were obtained for both methanolate and ethanolate. DSC and TG thermograms of these crystals are shown in Fig. 2. In DSC thermograms, a broad endothermic peak with double-peaks at 135 and 151 °C was observed for methanolate. Meanwhile, a sharp endothermic peak at 135 °C with a minor shoulder at 141 °C was observed for ethanolate. The temperatures where weight losses were observed in TG thermograms corresponded well to the respective endothermic events in DSC, indicating that those endothermic events in DSC were due to the respective

alcohol desolvation from both crystals. The weight losses in methanolate and ethanolate were 5.02 and 6.72%, respectively. Taking the results of X-ray crystal analysis into account, it appears reasonable to assume that both alcohates are the 1 : 1 stoichiometric solvates of the compound with the respective alcohols. Hot-stage microscopic observation indicated that desolvation in both alcohates accompanied melting of the crystal. Unlike both the alcohates, the ansolvate exhibited no thermal change in DSC and TG until the temperature reached the sharp endothermic peak at 220 °C caused by the melting of the crystal, followed by an exothermal peak caused by decomposition. In the DSC thermograms of both alcohates, no endothermic peaks were observed at around 220 °C, suggesting that crystal formation from the desolvated alcohates after liquidization did not occur at the heating rate of 5 °C/min.

IR Spectroscopy Figure 3 shows IR spectra of the methanolate, ethanolate, and ansolvate. The strong absorption bands at around 1650 cm⁻¹ assigned to the carbonyl stretching vibration and at around 2870 and 2960 cm⁻¹ assigned to the C–H stretching vibrations of methyl groups were commonly observed in the three crystal forms. No clear

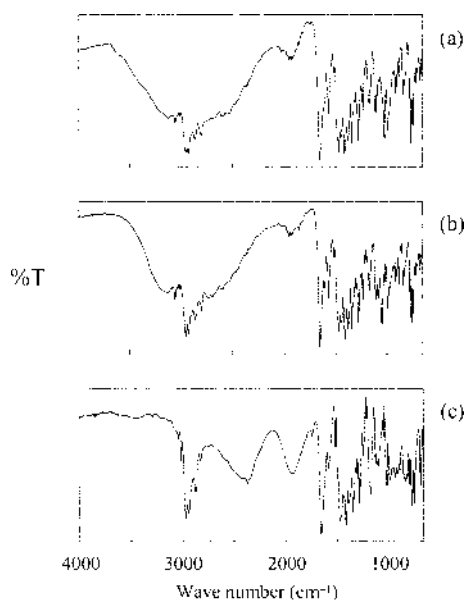


Fig. 3. IR Spectra of PNU-97018 Methanolate (a), Ethanolate (b), and Ansolvate (c)

absorption band expected at $3300\text{--}3500\text{ cm}^{-1}$ due to the free N–H stretching vibration of the tetrazole secondary amine was observed with any of the three crystal forms. The broad absorptions at $2500\text{--}3300\text{ cm}^{-1}$ evident in both alcoholates when compared with the ansolvate were similar to those typically observed in carboxylic acid dimers,¹⁵ suggesting strong intermolecular hydrogen bonding caused by the constituent alcohols. Unlike alcoholates, the ansolvate showed a broad and strong absorption band at around 2400 cm^{-1} assigned to N–H stretching vibration of ammonium salt, presumably resulting from the protonation of the N6 atom of the imidazole ring caused by the intermolecular hydrogen bonding with the tetrazole ring.

Molecular and Crystal Structures The crystal data of methanolate, ethanolate, and ansolvate are shown in Table 1. The displacement ellipsoid plots of the compound molecule in the methanolate, ethanolate, and ansolvate are shown in Figs. 4, 5, and 6, respectively. The imidazole rings of the compound in those crystals were all planar with the maximum deviation of $0.007(2)\text{ \AA}$ for methanolate, $0.005(2)\text{ \AA}$ for ethanolate, and $0.004(5)\text{ \AA}$ for ansolvate at the respective C15 atoms. The fused neighboring pyridazinone rings were all similarly distorted as seen in the deviations of N7 and N8 atoms (0.078 and 0.794 \AA for methanolate, 0.105 and 0.807 \AA for ethanolate, and 0.118 and 0.823 \AA for ansolvate, respectively) from the least-squares plane that consists of the C20, C21, C22, and C23 atoms. The two phenyl rings and the tetrazole ring in the biphenyltetrazole moiety were all planar for the compound molecules in the three different crystals, with maximum deviations of $0.010(2)$, $0.007(2)$, and $0.002(2)\text{ \AA}$ with methanolate, $0.013(2)$, $0.010(2)$, and $0.003(2)\text{ \AA}$ with ethanolate, and $0.003(6)$, $0.013(4)$, and $0.001(4)\text{ \AA}$ with ansolvate, for the C4, C9, and N1 atoms, respectively.

Although both alcoholates had similar dihedral angles between two phenyl rings in the biphenyltetrazole moiety (46.0° for methanolate and 46.3° for ethanolate), the anso-

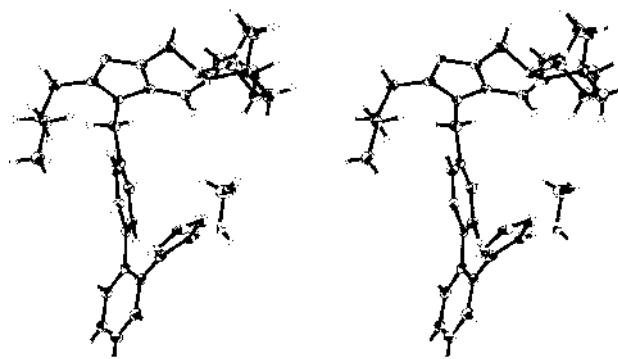


Fig. 4. Stereo View of the PNU-97018 Methanolate

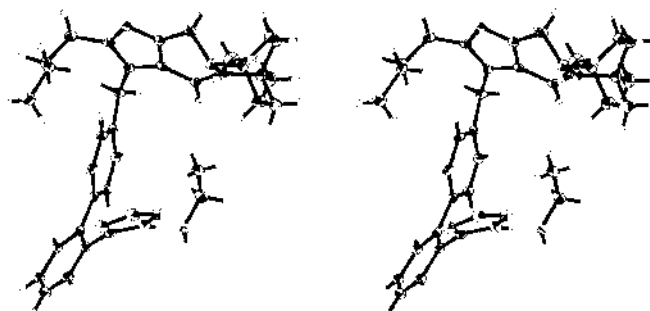


Fig. 5. Stereo View of the PNU-97018 Ethanolate

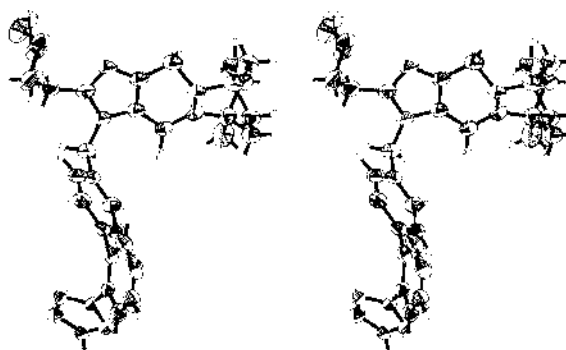


Fig. 6. Stereo View of the PNU-97018 Ansolvate

vate had a slightly larger dihedral angle of 52.2° . This was also true for the dihedral angles between the tetrazole ring and the neighboring phenyl ring (53.6° for methanolate, 53.3° for ethanolate, and 55.7° for ansolvate). These results were comparable with the respective dihedral angles of 45.8° and 58.8° reported by Shin *et al.*⁸) for a similar compound with a biphenyltetrazole moiety.

The torsion angles C21–N5–C14–C11 and N5–C14–C11–C10 around the methylene bridge were $72.1(2)^\circ$ and $21.02(2)^\circ$ for methanolate, $74.2(3)^\circ$ and $26.7(3)^\circ$ for ethanolate, and $74.5(4)^\circ$ and $65.9(4)^\circ$ for ansolvate, respectively, indicating that the positions of the biphenyl moieties toward the respective central heterocyclic rings in methanolate, ethanolate, and ansolvate are almost the same, and that the ansolvate has a different rotational conformation of the biphenyltetrazole moiety around the C11–C14 bond from both alcoholates. Figures 4–6 illustrate the difference in the

Table 2. Intermolecular Hydrogen Bond Distance

Crystal	Proton donor	Proton acceptor	Distance (Å)
Methanolate	Tetrazole (N1)	MeOH (O)	2.653 (2)
	MeOH (O)	Imidazole (N6)	2.764 (2)
Ethanolate	Tetrazole (N1)	EtOH (O)	2.682 (3)
	EtOH (O)	Imidazole (N6)	2.792 (3)
Ansolvate	Tetrazole (N2)	Imidazole (N6)	2.688 (5)

relative orientation of the tetrazole ring toward the central heterocyclic rings between alcoholates and ansolvate. The crooked molecular conformation of the compound in the methanolate and ethanolate drew their tetrazole rings close to the central heterocyclic rings, whereas in the ansolvate the tetrazole ring was at the remote position from the central heterocyclic rings, indicating more stretched molecular conformation than those of the alcoholates. The torsion angles of N5–C15–C16–C17 and N6–C15–C16–C17 were 74.4 (2)° and –103.3 (2)° for methanolate, 77.1 (3)° and –101.2 (3)° for ethanolate, and –78.5 (5)° and 97.0 (5)° for ansolvate, respectively, demonstrating that the orientation of the *n*-butyl side chain toward the imidazole plane is opposite between alcoholates and ansolvate. This indicates that the *n*-butyl side chain of the compound molecule of both the alcoholates bends and comes up to the same side of the imidazole plane as the biphenyltetrazole moiety, while that of ansolvate bends to the opposite side of the imidazole plane, as shown in Figs. 4–6. Part of the *n*-butyl side chain (the C18 and C19 atoms) of the compound molecule in ansolvate is disordered, as seen in Fig. 6, with an equal occupancy suggesting the flexibility of the *n*-butyl side chain.

Although the position of the hydrogen atom in the tetrazole ring bearing an acidic characteristic was at N1 for both the alcoholates, the compound molecule in the ansolvate crystal had the hydrogen atom at the N2 position. As shown in Table 2, the hydrogen atom of N1 in the tetrazole ring of the compound molecule in each alcoholate formed a hydrogen bond with the oxygen atom of the alcohol, as shown in Figs. 4 and 5. The hydroxyl hydrogen atom of the solvated alcohol further formed another hydrogen bond with the nitrogen atom (N6) of another molecule to develop the intermolecular hydrogen bond sequence shown in Figs. 7 and 8. An intermolecular hydrogen bond between the N2 atom of the tetrazole ring and the N6 atom of the imidazole ring was observed to form an intermolecular hydrogen bond sequence in the ansolvate crystal, as shown in Fig. 9. The hydrogen at N2 in the tetrazole ring of ansolvate probably has a conformational advantage in forming the intermolecular hydrogen bond sequence. The direct intermolecular hydrogen bonding in ansolvate is considered to have slightly ionic bonding characteristics because of the acidity of the hydrogen atom in the tetrazole ring and the basic nitrogen atom (N6) of the imidazole ring, explaining the probable ammonium ion formation at the nitrogen atom (N6). This is in good agreement with the characteristic IR absorption band at around 2400 cm⁻¹.

The crystal packing of methanolate and ethanolate are shown in Figs. 10 and 11, respectively, illustrating alcohol-mediated hydrogen bond sequences through the crystal along the *a*-axis. The methanolate and ethanolate were found to

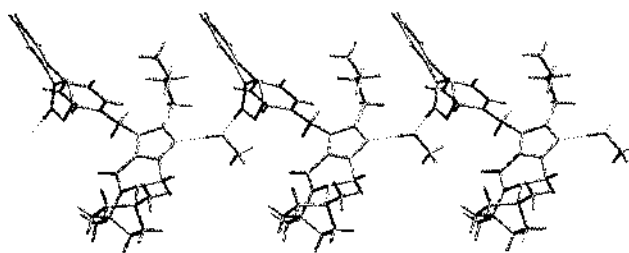


Fig. 7. Intermolecular Hydrogen Bonding Sequence in the PNU-97018 Methanolate Crystal

The dotted lines indicate hydrogen bonds.

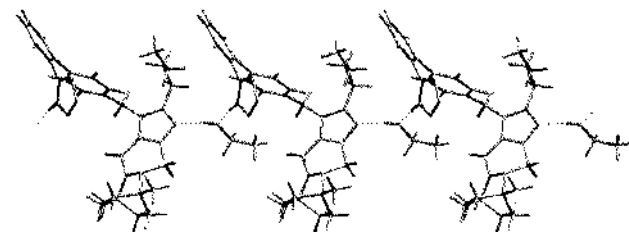


Fig. 8. Intermolecular Hydrogen Bonding Sequence in the PNU-97018 Ethanolate Crystal

The dotted lines indicate hydrogen bonds.

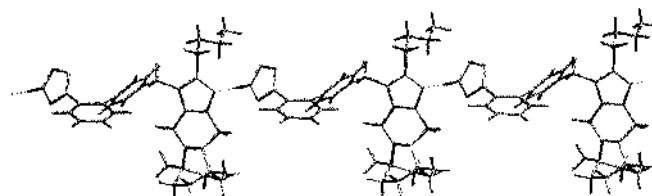


Fig. 9. Intermolecular Hydrogen Bonding Sequence in the PNU-97018 Ansolvate Crystal

The dotted lines indicate hydrogen bonds.

have almost identical crystal packing. The difference in the molecular size between methanol and ethanol had basically no influence upon the location of alcohol oxygen in the crystal, due to the preference for the hydrogen bond formation. Also, tunnel-like structures accommodating alcohol as the guest molecule were observed in methanolate and ethanolate when the molecules were viewed down the *c*-axis toward the *a*–*b* plane, as shown in Figs. 10 and 11. The alcohol molecules might be easily removed through the tunnel upon heating. The cavity dimensions of the cross-section of the tunnel-like structure were compared between methanolate and ethanolate (Fig. 12). No significant differences in the cavity dimensions between these alcoholates were seen.

It would be of interest to investigate the effect of more bulky alcohol molecules on the cavity formation and hence on the crystal packing. Figure 13 illustrates the crystal packing of the ansolvate with the hydrogen bond sequences. The molecular arrangement was different from those of alcoholates, as expected. The hydrogen bonds directly linked between the molecules, as depicted by the dotted lines in Fig. 13, ran almost parallel along the *b*-axis to create a wall-like network with thickness of *ca.* 14 Å, stacking on the *b*–*c* plane to develop the layer structure. Hydrogen bonding in the alcoholates and the ansolvate seems to play a dominant role

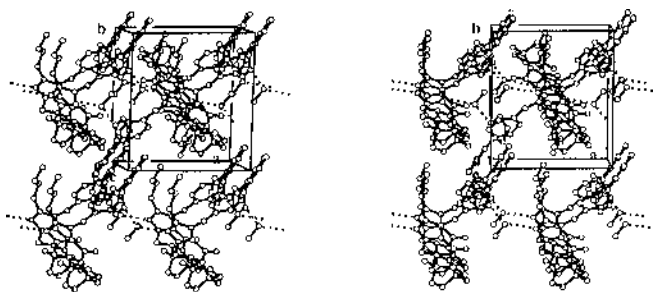


Fig. 10. Stereo View of Molecular Packing of PNU-97018 Methanolate Projected from the *c*-Axis

The dotted lines indicate hydrogen bonds. Hydrogen atoms are omitted for clarity.

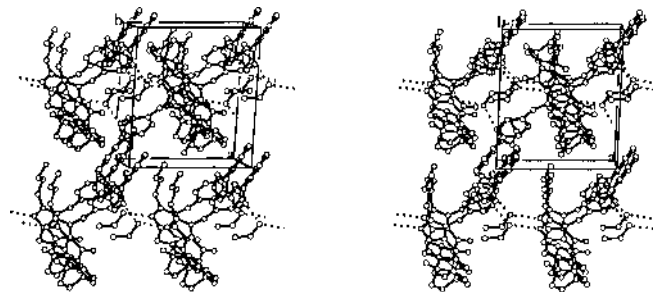
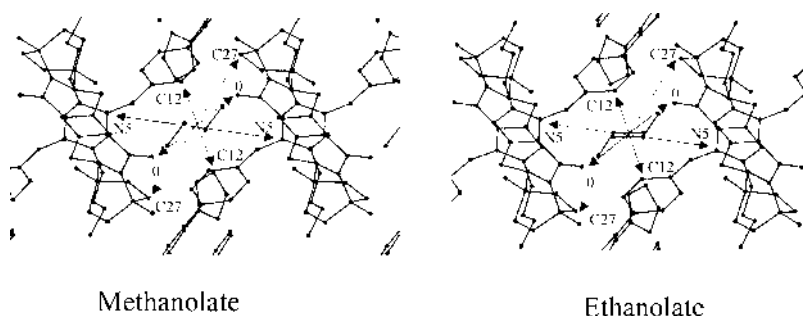


Fig. 11. Stereo View of Molecular Packing of PNU-97018 Ethanolate Projected from the *c*-Axis

The dotted lines indicate hydrogen bonds. Hydrogen atoms are omitted for clarity.



Distance between Atoms	Methanolate (Å)	Ethanolate (Å)
O.....O	5.46	5.63
C12.....C12	4.46	4.39
N5.....N5	8.33	8.41
C27.....C27	12.01	12.82

Fig. 12. Cross-Sectional Cavity Size of the Tunnel-Like Structures of PNU-97018 Methanolate and Ethanolate

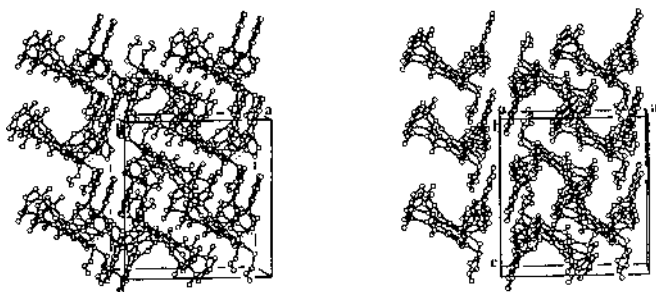


Fig. 13. Stereo View of Molecular Packing of PNU-97018 Ansolvate Projected from the *b*-Axis

The dotted lines indicate hydrogen bonds. Hydrogen atoms are omitted for clarity.

in arranging each molecule in an ordered sequence. However, further ordered structures beyond the hydrogen bond sequences in the crystal packing of the alcoholates and ansolvate (Figs. 10, 11, 12) is presumably formed by other intermolecular interactions.

Conclusions

In this study, we demonstrated the crystal structure of the ansolvate, methanolate, and ethanolate of the compound by X-ray crystallography to investigate the effect of alcohol solvation on the molecular and crystal structure of the com-

pound. Major differences were observed in the molecular conformation and in the molecular arrangement that constituted the crystal structure between the alcoholates (methanolate and ethanolate) and the ansolvate, as expected from the high conformational flexibility in this class of compounds.⁹⁾ The hydrogen bond sequence was considered to be a major crystal structure constituent for the alcoholates and the ansolvate, although an alcohol molecule worked as a mediator to connect two compound molecules in methanolate and ethanolate. The methanolate and ethanolate had quite similar crystallographical characteristics, including the tunnel-like structure in which alcohol molecules were held by hydrogen bonding.

Acknowledgments The authors are grateful to Miss Yuko Kawakita for technical assistance.

References and Notes

- 1) Morita O., Kushida H., Kunihara M., *J. Cardiovasc. Pharmacol.*, **25**, 880—887 (1995).
- 2) Kushida H., Nomura S., Morita O., Harasawa Y., Suzuki M., Nakano M., Ozawa K., Kunihara M., *J. Pharmacol. Exp. Ther.*, **274**, 1042—1053 (1995).
- 3) Duncia J. V., Carini D. J., Chiu A. T., Johnson A. L., Price W. A., Wong P. C., Wexler R. R., Timmermans P. B. M. W. M., *Med. Res. Rev.*, **12**, 141—191 (1992).
- 4) Kubo K., Inada Y., Kohara Y., Sugiura Y., Ojima M., Itoh K., Furukawa Y., Nishikawa K., Naka T., *J. Med. Chem.*, **36**, 1772—1784

- (1993).
- 5) Bradbury R. H., Allot C. P., Dennis M., Fisher E., Major J. S., Masek B. B., Oldham A. A., Pearce R. J., Rankine N., Revill J. M., Roberts D. A., Russell S. T., *J. Med. Chem.*, **35**, 4027—4038 (1992).
 - 6) Mantlo N. B., Chakravarty P. K., Ondeyka D. L., Siegel P. K. S., Chang R. S., Lotti V. J., Faust K. A., Chen T.-B., Schorn T. W., Sweet C. S., Emmert S. E., Patchett A. A., Greenlee W. J., *J. Med. Chem.*, **34**, 2919—2922 (1991).
 - 7) De B., Winn M., Zydowsky T. M., Kerkman D. J., DeBernardis J. F., Lee J., Buckner S., Warner R., Brune M., Hancock A., Opgenorth T., Marsh K., *J. Med. Chem.*, **35**, 3714—3717 (1992).
 - 8) Shin W., Yoon T. S., Yoo S. E., *Acta Cryst.*, **C52**, 1019—1022 (1996).
 - 9) Heo Y. S., Yi K. Y., Yoo S. E., Shin W., *Acta Cryst.*, **C55**, 1345—1347 (1999).
 - 10) The temperature measured in case of ansolvate was estimated to be the most suitable condition for stabilizing the flexible *n*-butyl side chain, which exhibits various disordered conformations depending on the temperature.
 - 11) Altomare A., Burla M. C., Camalli M., Cascarano G. L., Giacovazzo C., Guagliardi A., Moliterni A. G. G., Poridori G., Spagna R., *J. Appl. Cryst.*, **32**, 115—119 (1999).
 - 12) Beurskens P. T., Admiraal G., Beurskens G., Bosman W. P., de Gelder R., Israel R., Smits J. M. M., The DIRDIF-94 program system. Technical Report of the Crystallography Laboratory, University of Nijmegen, the Netherlands.
 - 13) teXan for Windows: Crystal Structure Analysis Package, Molecular Structure Corporation (1997).
 - 14) Cambridge Crystallographic Data Centre registration numbers for ansolvate, methanolate, and ethanolate are CCDC179730, CCDC179731, and CCDC179732, respectively.
 - 15) Silverstein R. M., Webster F. X., "Spectrometric Identification of Organic Compounds," 6th ed., John Wiley & Sons, New York, 1998, p. 107.